Arch. Metall. Mater. **66** (2021), 2, 367-372

DOI: 10.24425/amm.2021.135867

JIAYAN LI[1,2*], BENSON KIHONO NJUGUNA[1,2], PING NI[1,2], LIANG WANG[1,2], YI TAN[1,2]

RESEARCH ON DISTRIBUTION AND MORPHOLOGY OF PRIMARY Si UNDER THE EFFECT OF DIRECT CURRENT

A source of pure silicon was added into an alloy refining system during a refining process with the application of a direct electric current. The effect of the temperature difference between the graphite electrodes and the alloy was decreased. The temperature increase value (ΔT) of the Al-28.51wt.%Si alloy sample caused by Joule heating was calculated by weighing the mass of primary silicon. When the current density was 5.0×10^5 A/m^2, the overall temperature increase in the alloy was about 90°C regardless of the alloy composition. Adequate silicon atoms recorded the footprint of the electric current in the alloy melt. The flow convection generated by the electric current in the melt during the solidification process resulted in the refinement of primary silicon. The Fe impurity content in alloy refining without the electric current density was 2.16 ppm. However, it decreased to 1.27 ppmw with the application of an electric current density of 5.0×10^5 A/m^2.

Keywords: Silicon source, direct current, Joule heating, Si morphology, Fe impurity

1. Introduction

Researchers have focused on the application of current processing to strengthen alloy solidification and crystal growth for many years. At present, electric current processing was important in changing the alloy solidification process [1], grain growth [2], and solute or inclusions distribution [3]. With the improvement of the mechanical properties of the alloy, the effect of electric current on the refinement of grain size has been well verified. Researchers have carried out a large number of experiments on the solidification process of metal-based alloys such as Sn, Zn, Al, and Fe, and found that the grain size has been significantly changed under the influence of current [4-8]. Some researchers have observed the crystal growth under the influence of current during the alloy directional solidification [9]. The results show that the application of current can promote the stability of the solid-liquid interface, reduce the primary crystal spacing, and change the crystal morphology. Jiang et al. [10] investigated the effect of pulsed current on the solidification of immiscible alloy. It is believed that pulsed current can affect the formation of microstructures by changing the nucleation behavior of precipitated droplets. When the precipitated droplets have a higher conductivity than the matrix, pulse current can enhance the rate of nucleation and promote the formation of dispersed microstructures. Basrnak et al. [11] studied the effect of direct current on the solidification process. The experimental results show that the effect of the direct current electric field increases the degree of supercooling during the solidification process and the size of the eutectic structure decreases significantly. Some researchers [12-15] have studied the effects of current on the electro-migration process. The results indicate that the force of electro-migration is derived from the momentum transfer from the conductive electron to the atom. The direction of the electromotive force is opposite to the direction of the electric field. The flow convection of alloy melt caused by the current drives the migration of silicon nuclei near the positive electrode to the middle of the alloy. The flow of the melt has a very important influence on the microstructure and macrostructure of the final solidified structure and segregation behavior [16].

In summary, the electric current has an effect on the solidification process and the solute transport process in front of the solid-liquid interface, resulting in the microstructure change of the alloy. Joule heating effect [17], Peltier effect [18], and electro-migration [19] played a significant role in this effect.

However, due to the complexity of the electric current effect, the research work of the ideal solidification structure is still

[1] DALIAN UNIVERSITY OF TECHNOLOGY, SCHOOL OF MATERIALS SCIENCE AND ENGINEERING, NO. 2 LINGGONG ROAD, GANJINGZI DISTRICT, DALIAN 116023, CHINA
[2] DALIAN UNIVERSITY OF TECHNOLOGY, KEY LABORATORY FOR SOLAR ENERGY PHOTOVOLTAIC SYSTEM OF LIAONING PROVINCE, DALIAN 116024, CHINA

* Corresponding author: lijiayan@dlut.edu.cn

© 2020. The Author(s). This is an open-access article distributed under the terms of the Creative Commons Attribution-NonCommercial License (CC BY-NC 4.0, https://creativecommons.org/licenses/by-nc/4.0/deed.en which permits the use, redistribution of the material in any medium or format, transforming and building upon the material, provided that the article is properly cited, the use is noncommercial, and no modifications or adaptations are made.

underway, and other influencing factors are also being studied continuously. The most active effect of electric current in alloy solidification is Joule heating which has been researched in our previous work [20]. The purpose of this paper is to further clarify the effect of electric current on the solid-liquid coexistence zone and the redistribution and growth of primary silicon in the melt by the fluid flow caused by direct electric current. Additionally, the actual temperature increase and the temperature distribution in the alloy have also been investigated.

2. Experimental methods

The initial composition of alloy was set to about Al-28.5 wt.%Si (liquid temperature is 800°C) with a low refining temperature. The master alloys were prepared by melting the Al (99.9wt%) in an alumina crucible under an argon atmosphere using an induction furnace. The alloys were cast into a quartz tube with 5 mm inner diameter by a vacuum filling technique and quenched in water to avoid macro-segregation.

To further study the effect of current on the distribution of primary silicon in the solid-liquid coexistence region, cylinder silicon was added as a silicon source at both ends of the alloy. They were located between the graphite electrodes and the alloy. The temperature of the alloy melt could be increased under the current thermal effect. Silicon atoms from the silicon source diffused into the melt to "magnify" and "record" the electric current thermal behavior. The schematic diagram of the experiment with silicon source addition is shown in Fig. 1.

It is proposed that the temperature of the alloy system is increased due to the Joule heating effect caused by the direct electric current during the solidification process. The silicon source will continue to diffuse into the alloy until reaching the saturation state. Finally, the maximum change of temperature caused by the Joule heating effect in the alloy can be obtained by calculating the loss of the silicon source at both ends by the acid etching method. The eutectic alloys (Al-11.7wt.%Si) with liquidus temperature of 577°C and two hypereutectic alloys (Al-21.2 wt.%Si, Al-28.5wt.% Si) with liquidus temperature of 700°C and 800°C, respectively, were studied as master alloys in this experiment. Firstly, the three alloys were heated to their liquidus temperature respectively. Next, the same electric current was applied as soon as they reached their liquidus temperature and held for 60min. Further, they were cooled along with the furnace cooling process until the alloys solidified completely. Finally, the electric current was cut off and samples were taken out for quenching treatment. The acid leaching process was used to obtain the silicon piece. Additionally, the effect of different current densities (5.0×10^5 A/m^2 and 1.0×10^6 A/m^2) was considered in this experiment.

3. Results and Discussion

3.1. Effect of electric current on the change of alloy temperature with the silicon source

A master alloy with a composition of Al-28.5%wtSi (liquid temperature is 800°C) was heated to 800°C at a rate of 6°C/min in a flowing argon atmosphere. Direct electric current with a density of 1.0×10^6 A/m^2 was applied to the alloy. The furnace temperature was maintained at 800°C for 120 min and then cooled to 450°C, below the eutectic temperature (577°C).

Due to higher resistivity, the graphite electrodes will produce more Joule heating than that in the alloy melt. Fig. 2 shows the cross-section of Al-28.5%wtSi samples with and without the silicon source. Without a silicon source and without applying an electric current during the solidification process (Fig. 2a), primary silicon is distributed uniformly in the alloy. However, a temperature gradient was developed with a higher temperature at both ends and a lower temperature in the middle when a current density of 1.0×10^6 A/m^2 was applied. When the melt solidified under this temperature gradient, primary silicon was gradually concentrated in the middle part of the alloy. These results have been presented in our previous work [20]. In the current work, two silicon sources were added at both ends of the master alloy.

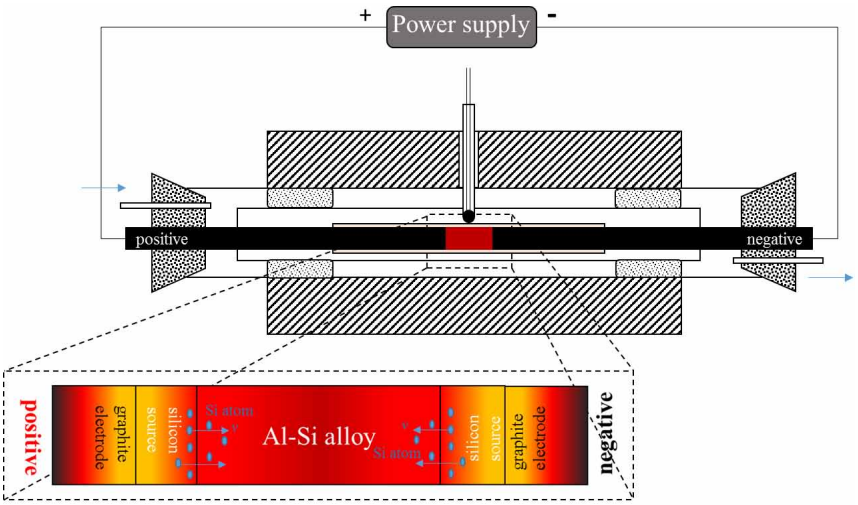

Fig. 1. Schematic diagram of the sample with silicon source addition

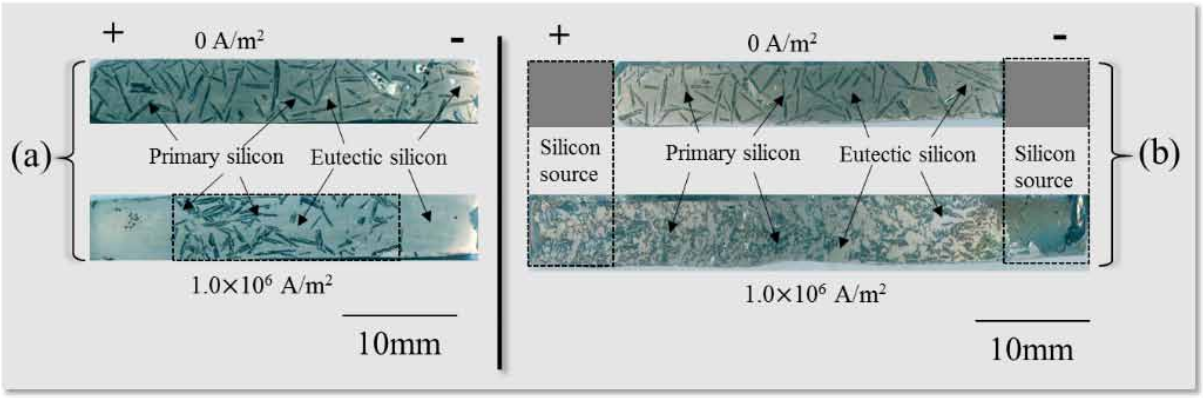

Fig. 2. Cross-section of Al-28.5%wtSi alloy samples without applied electric current and with the electric current density about 1.0×10^6 A/m^2. (a) without Si source (b) with Si source

The aggregation phenomenon disappeared when the silicon sources were added between the graphite electrodes and the alloy (Fig. 2b). Thus, the effect of temperature gradient in alloy caused by the different Joule heating of graphite electrodes and the alloy was removed.

Although the effect of temperature gradient was eliminated in the experiment, Joule heating of electric current is still the main factor that has a great influence on the solidification structure. to obtain the temperature change in alloys with the application of electric current, the eutectic alloy (Al-11.7wt.%Si) and two hypereutectic alloys (Al-21.2 wt.%Si and Al-28.5wt.% Si) with liquidus temperature of 577°C, 700°C, and 800°C respectively were studied as master alloys in this experiment. The different current densities (5.0×10^5 A/m^2 and 1.0×10^6 A/m^2) were applied to the alloys. The Si sources dissolved in the alloy due to the temperature increase caused by Joule heating. The calculated final liquidus temperature of each sample was compared with the initial liquidus temperature corresponding to the original alloy composition, as shown in Fig. 3. When the current density is 5.0×10^5 A/m^2, the temperature increase of the eutectic alloy (577°C) is about 90°C, which is close to that of the two hypereutectic alloys (700°C, 800°C) with the same current density treatment. When the current density was increased to 1.0×10^6 A/m^2, the temperature increase in the eutectic alloy and the two hypereutectic alloys was about 160°C, significantly higher than that with a current density of 5.0×10^5 A/m^2. It can be inferred that the temperature change caused by the Joule heating effect is independent of the ambient temperature of the furnace and alloy composition and is only related to the applied current density in the experiment.

The system voltage of hypereutectic alloys (Al-28.5wt.% Si) was also recorded during the cooling process and plotted as shown in Figure 4. According to Ohm's law, voltage changes reflect the resistance change of the entire system with a constant current. It is known that, below 1200°C, the conductivity of the graphite electrode increases with the increase of temperature. But this change is very small in reality. Therefore, the change in voltage mainly reflects the change in the internal resistance of the alloy sample. It can be seen that during crystallization and growth of primary silicon, the resistance of the alloy changes in a wavy manner. The solidification process began at the furnace temperature of 725°C and ended at 555°C with the current density of 5.0×10^5 A/m^2. When the current density was changed to 1.0×10^6 A/m^2, primary silicon solidified at the

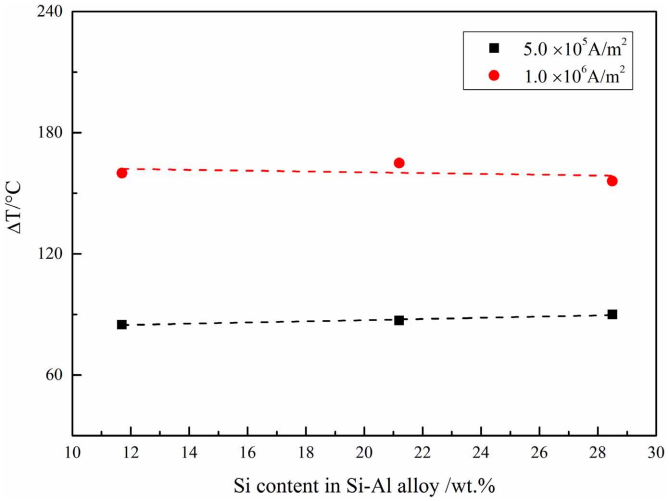

Fig. 3. Influence of alloy composition and current density on the temperature change of alloys

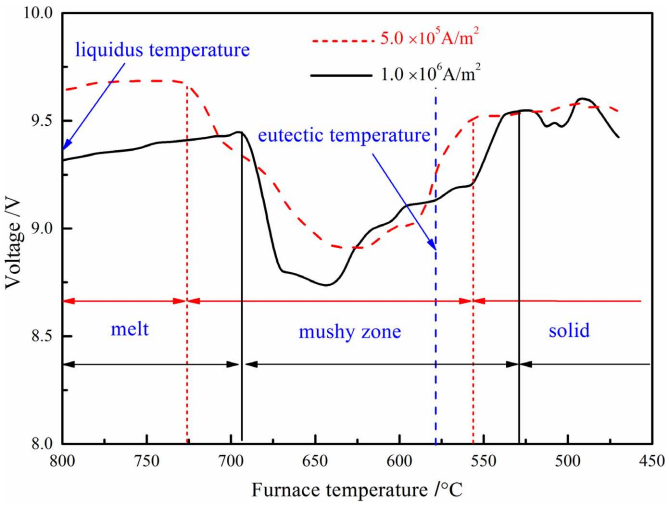

Fig. 4. Changes of system voltage along with temperature for the Al-28.5wt.%Si alloy sample

furnace temperature of 680°C and ended at 530°C. However, the liquidus temperature of an Al-28.5wt.% Si alloy sample is 800°C and the eutectic temperature is 577°C, indicating that the alloy sample temperature was different from furnace temperature. This confirms that the Joule heating resulted in the temperature increase of the alloy melt. And the temperature increase of the alloy melt was enhanced by the increase in the electric current density.

3.2. Effect of convection flow on the distribution and microstructure of primary Si

Fig. 5 shows the metallography of an Al-28.5wt.% Si sample with a current density of 1.0×10^6 A/m^2. The primary silicon advanced in the form of a "wave" from the positive electrode to the negative electrode end of the melt. Therefore, it can be inferred that the applied current caused the convection of the alloy melt along its direction, driving the silicon nuclei near the positive electrode to the middle of the alloy. The silicon atoms kept diffusing into the melt in the electric current direction, resulting in less consumption of the silicon source at the negative terminal relative to the positive one. From the cross-section of the sample, it is evident that the silicon source at the positive electrode terminal is melted in a larger amount than that at the negative electrode terminal.

During the furnace cooling process, the primary silicon in the alloy sample grows in a long strip shape and evenly distributes in the sample without the application of electric current (Fig. 6a). As shown in Fig. 6b and c, the initial silicon dendrites precipitating in the melt were refined by the current application with a current density of 5.0×10^5 A/m^2 and 1.0×10^6 A/m^2 respectively.

Classical heterogeneous nucleation theory indicated that the nucleation rate can be calculated using the following equation [11]:

$$N \approx \text{Const.}\left(\frac{D_L}{a^2}\right)\exp\left[\frac{-16\pi\gamma_{LS}T_f V_m f(\theta)}{3kT\Delta H_f^2\Delta T^2}\right] \qquad (1)$$

Where: N is nucleation rate; D_L is the liquid diffusivity; a is the jump distance; γ_{LS} is the liquid-solid interfacial energy; T_f is the equilibrium freezing temperature; V_m is the molar volume; $f(\theta)$ is a shape factor for heterogeneous nucleation; ΔH_f is the enthalpy of freezing and ΔT is the degree of supercooling.

The electric current can directly affect one or more of the parameters in the above expression for the nucleation rate during solidification. It is proposed that a reduction in the free energy difference between the liquid and solid states or an increase in the liquid-solid interfacial energy could increase the nucleation rate. Thus, with the application of electric current in the solidification process, the nucleation of primary silicon crystals is increased, leading to a refined structure.

The primary silicon near the positive electrode and negative electrode part were compared, as shown in Fig. 6. #1 and #2 represent the morphology of primary silicon at both ends of the sample without electric current application. #3 and #5 are the morphology of primary silicon in the positive region with the varying current application about 5.0×10^5 A/m^2 and 1.0×10^6 A/m^2 respectively. The primary silicon exhibits a flocculent structure. #4 and #6 show the morphology of primary silicon in the negative electrode region. It can be seen that the primary silicon was thicker in the negative electrode region than in the positive region. There is a potential difference in the solid-liquid interface due to the different conductivity between the solid and liquid phases [21]. Consequently, additional heat is generated when the current flows through the interface. Moreover, when the current flows from the liquid phase to the solid phase, the heat is released whereas it is absorbed when the current flows in the opposite direction. The cooling rate of the positive electrode was faster than that of the negative electrode, thus the primary crystal silicon near the negative electrode grows.

Due to the existence of constitutional supercooling on the solid-liquid interface during alloy refining, the primary silicon grows into the melt in a strip or petal-like shape. However, with the application of direct electric current, a liquid flow was generated in a liquid phase along the current direction, resulting in a change in the structure and distribution of the primary silicon. The arc shapes appeared in the solid-liquid growth interface. Fig. 7a and b show the morphology of primary silicon with a current density of 5.0×10^5 A/m^2 and 1.0×10^6 A/m^2 respectively. Due to higher resistance in the liquid phase than in the solid-phase, more electric current will flow through the

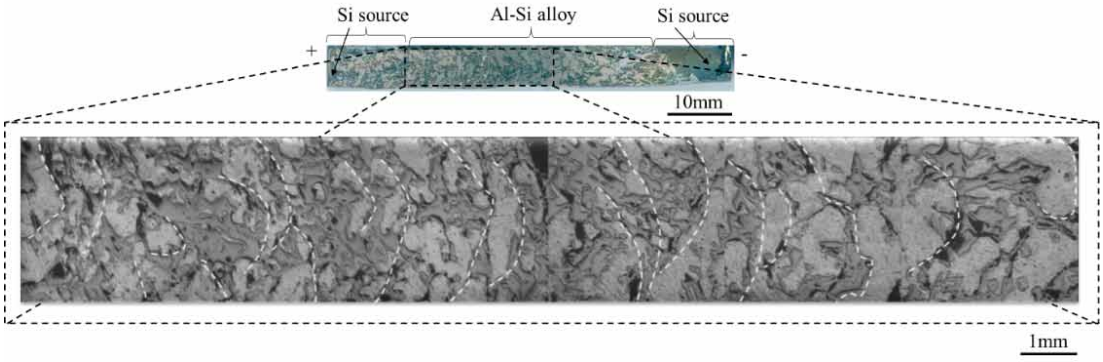

Fig. 5. Metallographic microscope picture of Al-28.5wt.%Si alloy sample with a current density of 1.0×10^6 A/m^2

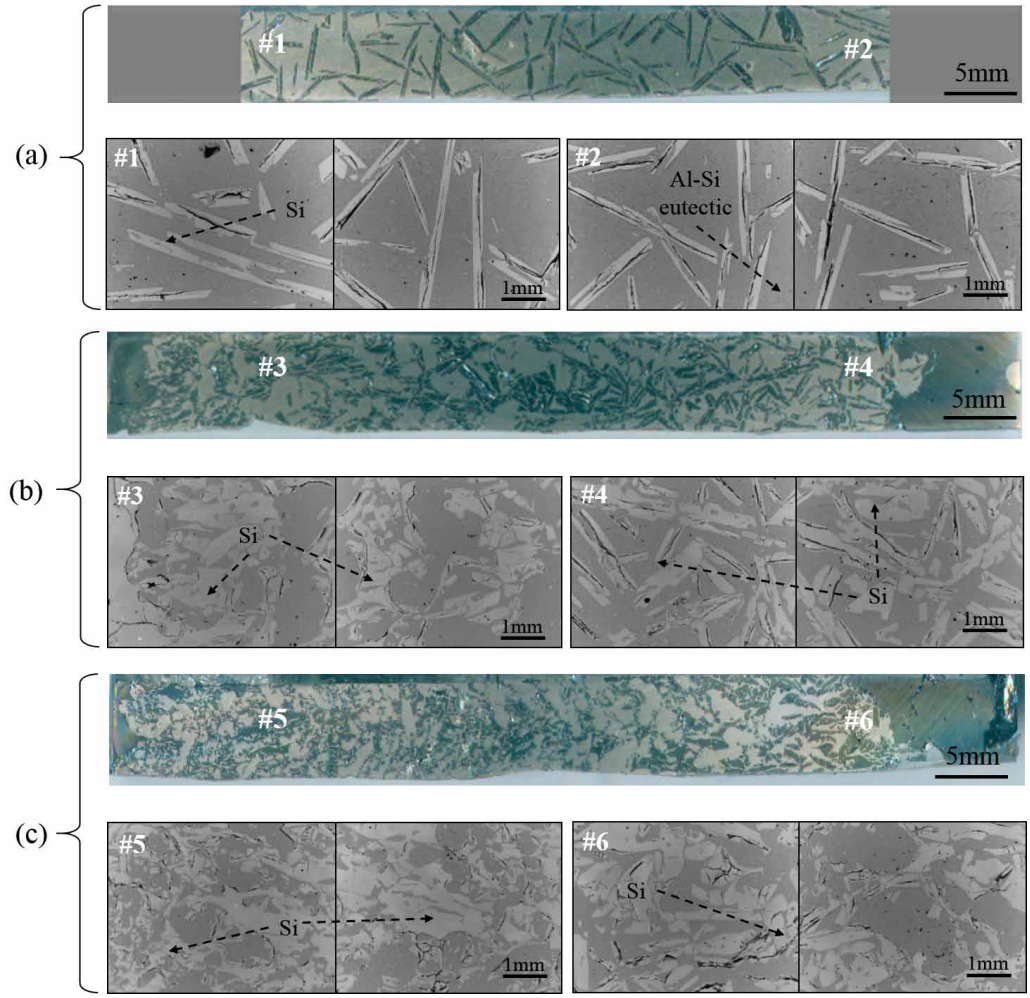

Fig. 6. SEM of primary silicon distribution for the Al-28.5wt.%Si alloy sample near the electrode location with addition of silicon source (a) 0 A/m^2, (b) 5.0×10^5 A/m^2, (c) 1.0×10^6 A/m^2

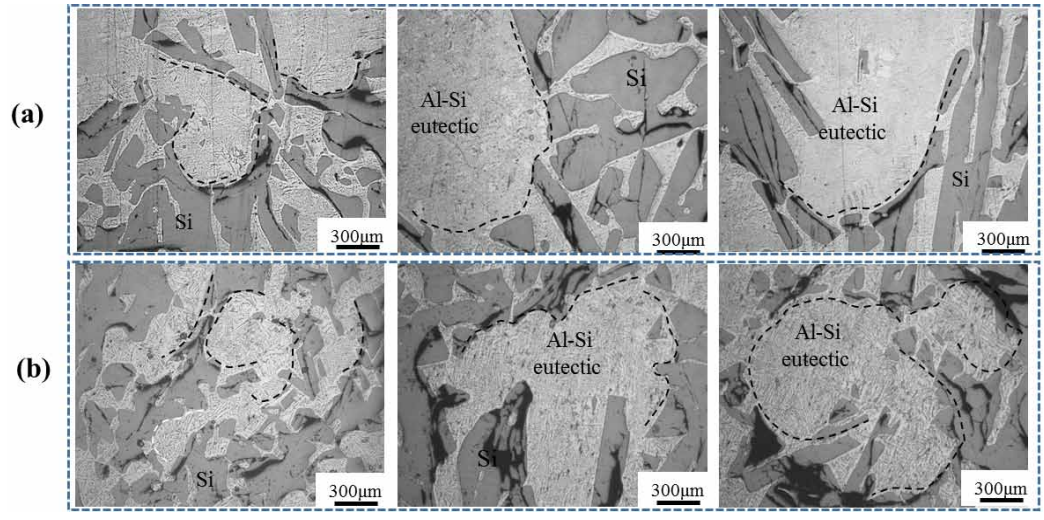

Fig. 7. The effect of convection on the boundary of primary silicon in the Al-28.5wt.%Si alloy sample (a) 5.0×10^5 A/m^2, (b) 1.0×10^6 A/m^2

solid phase, resulting in a higher temperature increase in the solid phase. Therefore, the uneven temperature in the local area could also cause convection in the melt. This convection in the melt could, subsequently form an arc boundary of primary silicon.

3.3. Effect of electric current on the separation of the Fe impurity in the primary silicon

The Fe concentration was analyzed by using an inductively coupled plasma mass spectrometry (ICP-MS ELEMENT 2,

Thermo Electron, Bremen, Germany). Fig. 8 shows the content of Fe impurity of primary silicon after treatment with varying electric current densities. It can be found that the Fe content in primary Si without application of electric current is 2.16 ppmw, while it becomes 1.27 ppmw with the electric current density of 5.0×10^5 A/m^2. As the electric current density increase to 1.0×10^6 A/m^2, the removal rate of Fe impurity remains. When the current density increases further to 1.5×10^6 A/m^2, the Fe impurity content increases sharply. It is shown that the electric current has a certain effect on the segregation behavior of Fe impurity in the refining process. When the current density is maintained at a low level, it can further strengthen the segregation process of Fe impurity based on the original alloy refining process. However, when the current density exceeds a certain value, its effects could be detrimental to the segregation process. Therefore, our research work needs to further explore the specific value of the reasonable current parameters.

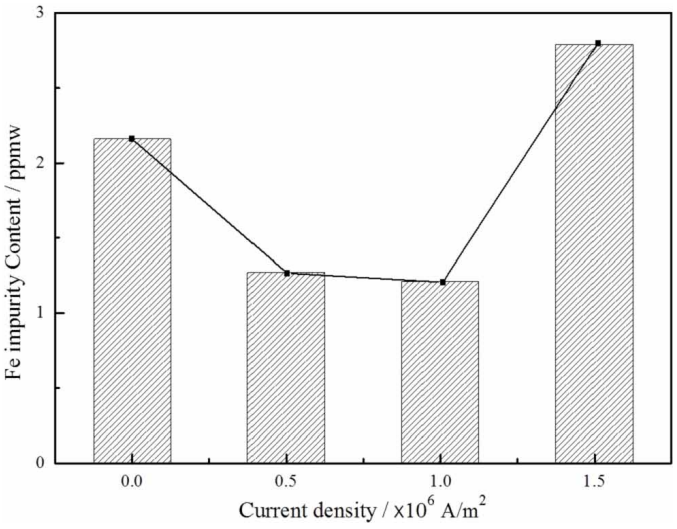

Fig. 8. Fe impurity content in the Al-28.5%wtSi alloy sample with different electric current density

4. Conclusions

(1) With the addition of silicon source, the effect of the temperature difference between graphite electrodes and the alloy sample was decreased when the current densities of 5.0×10^5 A/m^2 and 1.0×10^6 A/m^2 were respectively applied in the experiment. And the aggregation phenomenon disappeared in the microstructure of the alloy.

(2) When the current density was 5.0×10^5 A/m^2, the overall temperature increase of the eutectic alloy (577°C) was about 90°C, which is close to that of the two hypereutectic alloy (700°C, 800°C) with the same current density treatment. The temperature increase was about 160°C with the current density is 1.0×10^6 A/m^2. The result indicated that the temperature change caused by the Joule heating effect is independent of the furnace temperature and alloy compositions, which is related to current density.

(3) For the Al-28.5wt.%Si alloy sample, Fe impurity content in primary silicon without electric current is 2.16 ppmw, while it becomes 1.27 ppmw with the electric current density of 5.0×10^5 A/m^2. Electric current has a certain effect on the segregation behavior of the impurities in the refining process.

Acknowledgements

This program is financially supported by National Natural Science Foundation of China (Grant No. 51574057), and the Fundamental Research Foundation for the Central Universities (DUT19JC30).

REFERENCE

[1] B. Ban, Y. Li, Q. Zuo, T. Zhang, J. Chen, S. Dai, J. Mater. Process. Technol. **222**, 142-147 (2015).
[2] L.N. Brush, B.T. Murray, J. Cryst. Growth **250**, 170-173 (2003).
[3] P.A. Nikrityuk, S. Ananiev, K. Eckert, et al., Magnetohydrodynamics **45**, 407-416 (2009).
[4] F.C. Robles Hernandez, J.H. Sokolowski, J. Alloys Compd. **426**, 205-212 (2006).
[5] H. Conrad, H. Cuo, F.A. Sprecher, Scripta Mater. **24**, 359-362 (1990).
[6] K. Vashchenko, D. Chernega, S. Vorobev, et al., Met. Sci. Heat Treat. **16**, 261-265 (1974).
[7] C. Song, Y. Guo, Y. Zhang, H. Zheng, M. Yan, Q. Han, Q. Zhai, J. Cryst. Growth **324**, 235-242 (2011).
[8] Z. Zhao, J. Wang, L. Liu, Mater. Manuf. Processes **26**, 249-254 (2011).
[9] W.D. Griffiths, D.G. McCartney, Mater. Sci. Eng. A, **216** (1), 47-60 (1996).
[10] H. Jiang, J. Zhao, C. Wang, X. Liu, Mater. Lett. **132**, 66-69 (2014).
[11] J. Basrnak, A. Sprecher, H. Conrad, Scripta Mater. **32**, 879-884 (1995).
[12] J. Tan, E.M. Ryan, J. Power Sources **323**, 67-77 (2016).
[13] Y. Zhang, H.S. Ding, S.Y. Jiang, R.R. Chen, J.J. Guo, Chian Foundry **7**, 241-247 (2010).
[14] W. Lu, S. Zhang, J. Li, Mater. Lett. **107**, 340-343 (2013).
[15] W.L. Wang, Z.Q. Li, B. Wei, Acta Mater. **59**, 5482-5493 (2011).
[16] R.E. Shaw, J.D. Verhoeven, Metall. Trans. **4**, 2349-2355 (1973).
[17] Z. Yin, D. Liang, Y. Chen, Y. Cheng, Q. Zhai, Trans. Nonferrous Met. Soc. China **23**, 92-97 (2013).
[18] P.W. Egolf, L. Gravier, T. Francfort, A.G. Pawlowski, G. Courret, M. Croci, Int. J. Refrig. **37**, 176-184 (2014).
[19] X. Li, F. Lu, H. Cui, X. Tang, Trans. Nonferrous Met. Soc. China **24** (1), 192-198 (2014).
[20] Y.J. Li, P. Ni, L. Wang, Y. Tan, Mater. Sci. Semicond. Process. **61**, 79-84 (2017).
[21] A.A. Wheeler, J. Cryst. Growth **100**, 78-88 (1990).